

## ULTRASONIC CHARACTERIZATION OF SURFACE AND SUB-SURFACE DEFECTS IN CERAMIC MATERIALS

A. Stockman, M. Lam and P.S. Nicholson  
Materials Science and Engineering Department  
McMaster University, Hamilton, Ontario, Canada

### INTRODUCTION

The ultrasonic testing of ceramic materials is a two headed problem. First, the defect must be detected and second it must be characterized. Interior defects as small as 5  $\mu\text{m}$  can be catastrophic as can surface cracks of less than a micrometer opening. There are a number of problems to be overcome in the detection of defects ultrasonically such as the amplitude of the ultrasonic signals and the maximum useful frequency of the ultrasound. These problems are being addressed by the development of high power, 100 to 200 MHz transducers and the improvement of electronics technology. This paper is concerned with the second problem, i.e. the characterization of defects and is divided into two parts, one concerned with interior defects and the second with surface defects. The common thread is the spectral analysis of the signals received from the defects.

### SUB-SURFACE DEFECTS

Sensible NDE of ceramics requires a database and such has been developed via model defects introduced into model ceramics. Glass was selected as the initial model matrix as defects therein can be optically characterized, facilitating interpretation of the ultrasonic signals therefrom. To start with, small bubbles 25 to 120  $\mu\text{m}$  diameter were imbedded in the glass. A standard 25 MHz focussed transducer was used in pulse echo mode for the experimental work and it became apparent that simple amplitude measurements of the backscattered signals contained too many extraneous factors to be used for sizing the voids. The signals were therefore transformed from time to frequency domain first via a spectrum analyzer and later by digitizing and fast Fourier transforming the signal in a computer. The latter facilitated quantification of the spectra.

The spectrum of the focussed signal from the top surface of the samples was used as reference thus ensuring that the in-focus sound-field at the defects would be sufficiently similar as to allow comparison between defects. To a close approximation the spectrum is Gaussian and so can be characterized by its frequency at maximum amplitude (FMA) and its full-width-at-half-maximum amplitude (FWHM). These same two parameters are those which can be measured from the backscattered magnitude spectra for comparison of signals from different defects.

In order to correlate the results, a mathematical model was developed. In 1954 Ying and Truell [1] and later Johnson and Truell [2] developed the physics of a continuous plane wave scattering from spherical obstacles. It is an analytic form which takes into account the material parameters of the host and defect (for inclusions). In view of the experimental approach it was necessary to modify the analysis to include a pulsed and focussed sound field. The sound field in the focal zone of a focussed transducer can be approximated as a plane wave [3] provided the scatterers are  $< 300 \mu\text{m}$  diameter. The Fourier decomposition of the pulse is achieved through a

Gaussian approximation used for the sample surface reflection. The resulting total equation for the backscattered ultrasound pressure at the transducer  $P_T$  as function of frequency,  $f$ , and defect radius,  $a$ , is given by:

$$P_T(f) = \frac{2\rho f}{c} a \exp[-ikz_f] \exp\left[-4\ln 2\left(\frac{f-f_0}{f_{FWHM}}\right)^2\right] \sum_{m=0}^{\infty} (2m+1)A_m(\rho_h, \rho_i, v_{Lh}, v_{Li}, v_{Th}, v_{Ti})$$

Here  $f_0$  is the frequency of maximum amplitude of the incoming signal and  $f_{FWHM}$  is the FWHM of the incoming signal. The terms  $A_m$  arise from the plane wave scattering equations of Ying and Truell and are themselves functions of the frequency, density,  $\rho_h$  and  $\rho_i$ , longitudinal sound velocity,  $v_{Lh}$  and  $v_{Li}$ , and transverse sound velocity,  $v_{Th}$  and  $v_{Ti}$ , where the subscripts h and i represent host and inhomogeneity parameters respectively. Thus it was possible to calculate the expected magnitude spectra for a range of void diameters in a glass matrix. The FMA and FWHM of the resultant calculated spectra as a function of void diameter are shown in Figure 1. It should be noted that the model most closely matches the smallest diameter of the oblate spheroidal voids in the direction of ultrasound propagation.

Following success with analysis of voids, spherical inclusions of zirconia and magnesia were imbedded in glass and the experiments were repeated. Figure 2 shows the resultant close correlation of theory and experiment. One sample shows a disparity and closer optical examination showed the MgO sphere had partially debonded from its glass matrix. The glass and crystallized glass investigations are described in more detail elsewhere [4].

Finally, having developed a database using glass, metallic Pt inclusions were included in opaque zirconia ceramics. The calculated and measured FMA and FWHM results are shown in Figure 3. The necessary material parameters for the zirconia were assembled by direct measurement. Those for platinum were taken from the literature [5]. The model is sensitive to parameter variation and this may be the source of discrepancy between the observed and calculated FWHM and FMA values.

Clearly the relationships between the FMA, FWHM and the defect diameter are non-linear. This is the result of the influence of the Franz wave that circumnavigates the inhomogeneity [6]. These waves appear in the time domain as trailing signals. In the frequency domain they produce resonances that result in either secondary peaks in the spectrum or broadening thereof.

## SURFACE DEFECTS

To model a surface breaking crack in a ceramic material, a glass bar was grooved on the underside, mounted on a large-barrel micrometer stage and cracked in two to the groove. The two mating pieces were moved together or parted under micrometer control simulating a crack

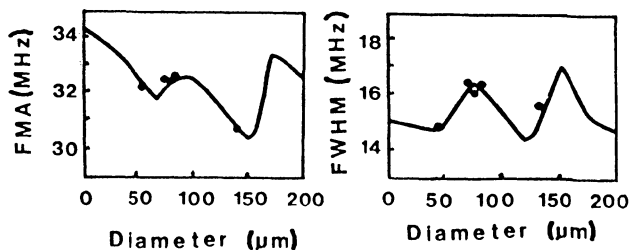


Fig 1. FMA and FWHM vs void diameter for bubbles in glass. the solid line represents the model calculations and the dots represent the smallest diameter of the spheroidal bubbles.

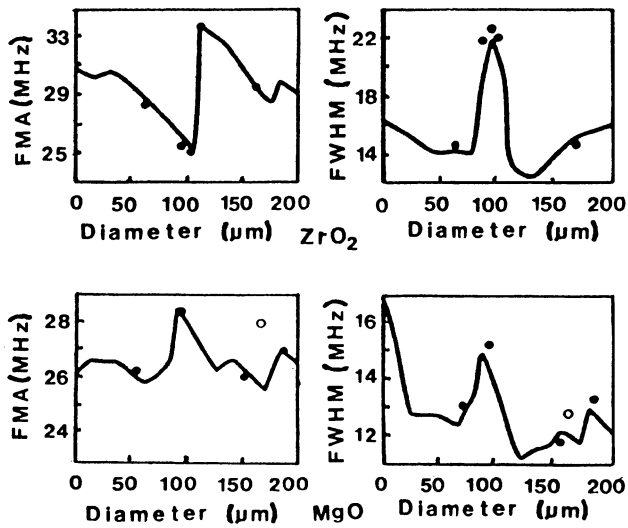


Fig. 2. FMA and FWHM vs diameter of spherical inclusions of zirconia and magnesia in glass. The type of glass was selected to match the thermal expansion of the inclusion. The hollow point represents a debonded inclusion.

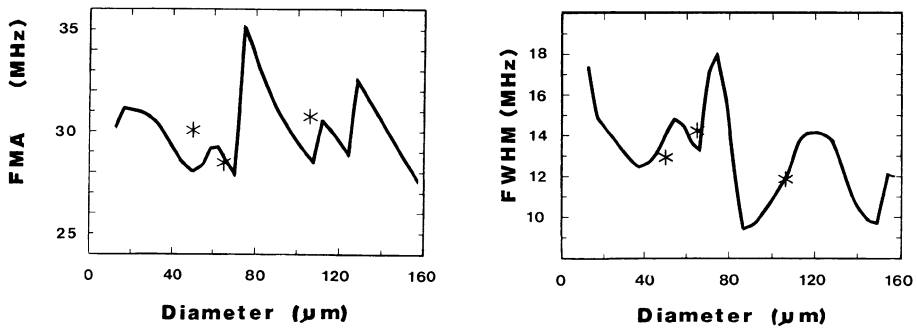


Fig. 3. FMA and FWHM vs diameter of Pt inclusion in zirconia. Asterisk patterns represent values recorded for data points.

opening. The same ultrasonic setup was used with the transducer tilted relative to normal incidence. The system analyzed is shown in Figure 4. The transducer was scanned across the crack and the signal amplitude maximized by focussing on the crack. This signal was then digitized and Fourier transformed to obtain the magnitude spectrum.

A theory was developed to compare calculated and experimental results. The net signal observed for a crack opening was taken to be the sum of the signal originating from the left side and that from the right side, delayed by a time,  $\Delta t$ , as given by:

$$\Delta t = \frac{2L \sin \theta}{C_w}$$

where  $L$  is the crack opening,  $\theta$  is the transducer tilt and  $C_w$  is the speed of sound in water. To measure the signal from each edge, the opposite side was moved out of the sound field and the transducer scanned to obtain the maximum signal which was then recorded digitally. It was found experimentally that the signals from each edge have approximately equal amplitudes but

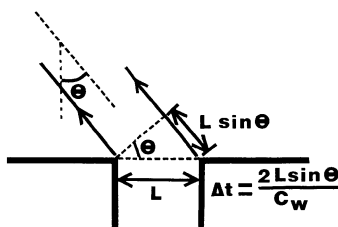


Fig. 4. Experimental configuration for crack width study

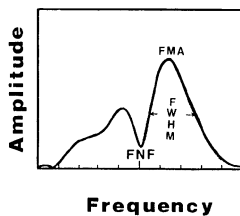


Fig. 5. Measured parameters of frequency spectra for crack studies.

reversed phase for a transducer tilt of 10-15 degrees. These angles were used in the experiments. A computer shifts the signal from the right edge and adds it to the signal from the left. The resultant composite signal is then Fourier transformed as shown in Figure 5

The characteristics of this magnitude spectra are the FMA, FWHM and the first null frequency (FNF) which is the frequency for which there has been signal cancellation resulting in a minimum in the spectrum. The left, right and summed time-domain signals are shown with their frequency spectra in Figure 6. The expected variations of FMA, FWHM and FNF from the model are plotted against crack opening for  $10^\circ$  incidence in Figure 7 and  $15^\circ$  incidence in Figure 8. The FNF data are fit by the curves down to the point where the null frequencies are beyond the frequency range of the transducer. The FMA data follows the model curves and is reasonably linear except on approaching the frequencies where the FNF is in the range of the main frequency component of the transducer. The minimum crack opening investigated was  $30 \mu\text{m}$ . Narrower openings are being achieved by a modified micrometer stage and will be investigated when available.

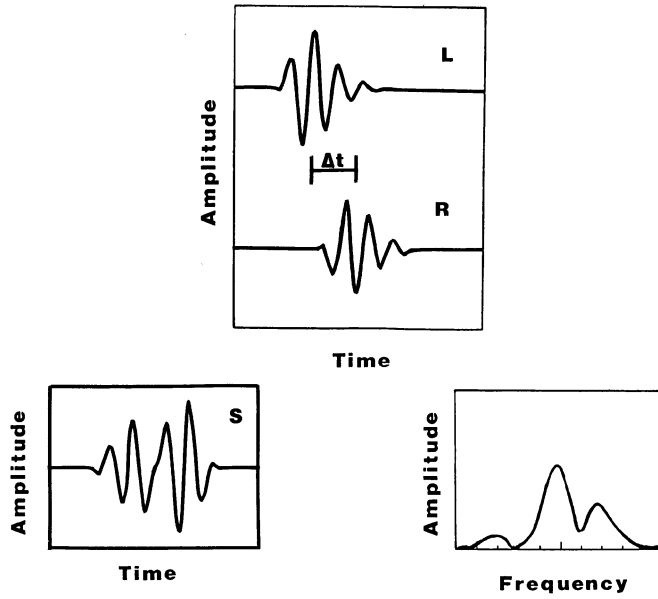


Fig. 6. Summing the signal from the left and right edges with a time delay  $\Delta t$ . Also showing the frequency spectrum of the resultant signal.

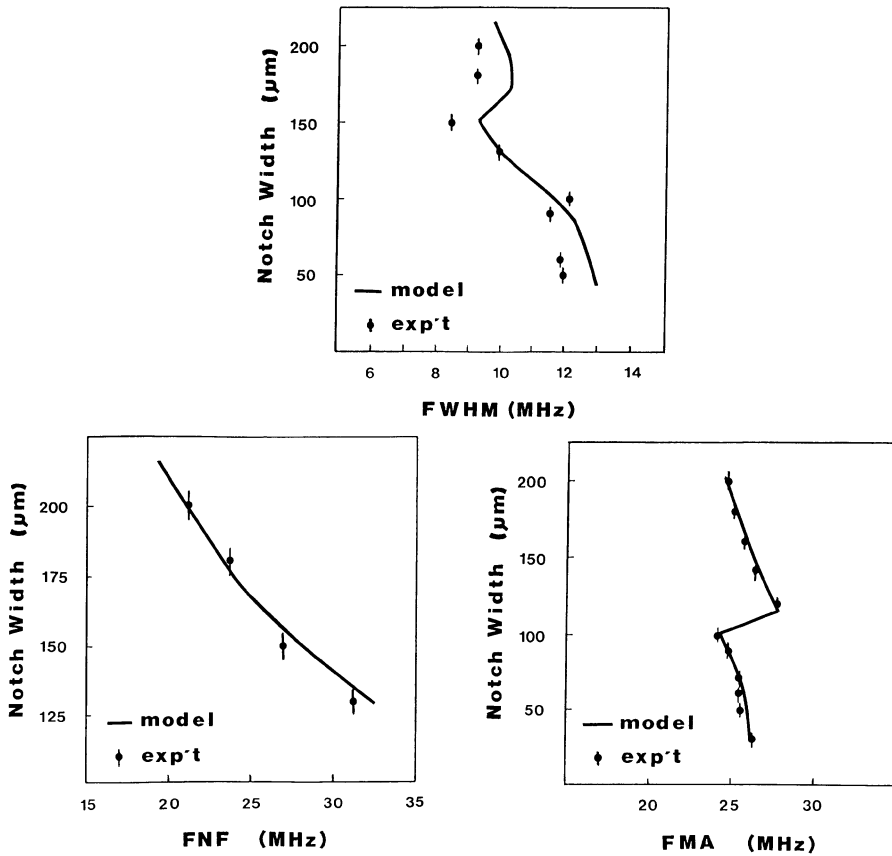


Fig. 7. FMA, FWHM and FNF as function of notch width for  $10^\circ$  incidence.

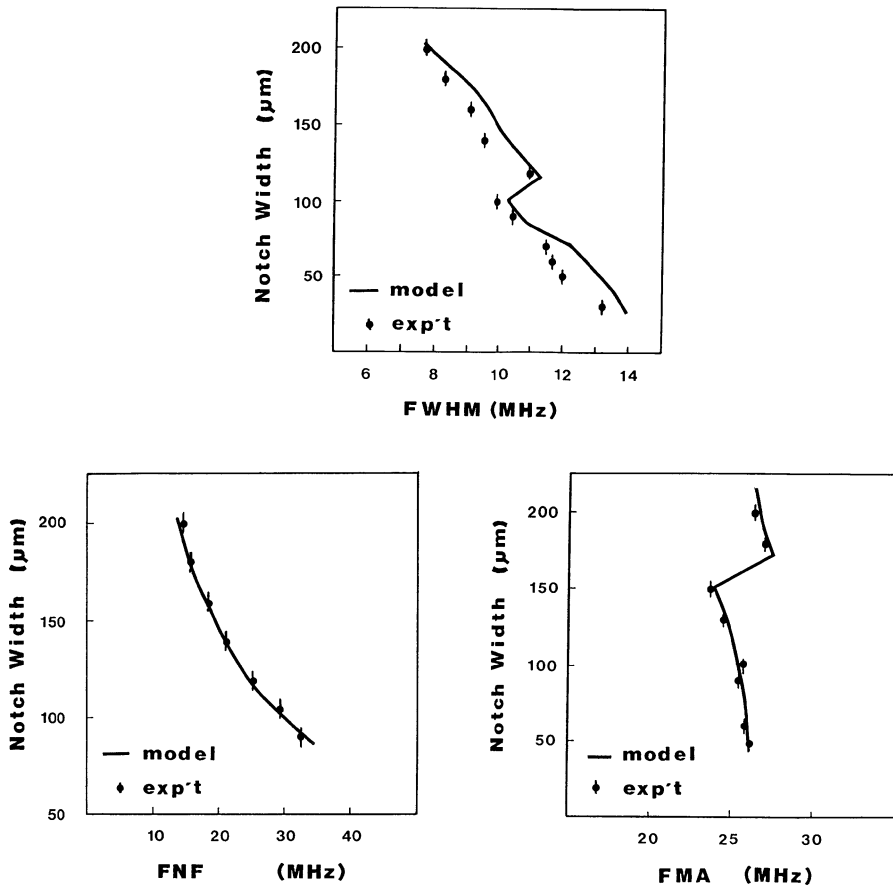


Fig. 8. FMA, FWHM and FNF as function of notch width for  $15^\circ$  incidence.

## CONCLUSIONS

The results of modelling and experimentally investigating surface and sub-surface defects in model ceramics using ultrasound are presented herein. A systematic database is developed starting with an optically-analyzable glass matrix before moving to a typical, opaque ceramic. The major features of the work are the simplicity and accuracy of the experimental design, the measuring of parameters from the defect frequency spectra and modelling ultrasound scattering for both types of defects. In the future internal defects will be scanned with multiple transducers of different frequencies to determine the sound velocity in and density of, the defects. Surface-breaking cracks with opening  $> 30 \mu\text{m}$  have been modelled and the model predictions of ultrasonic scattering therefrom shown to agree with experimental data. In the future, openings  $< 25 \mu\text{m}$  will be achieved and the interaction of sound waves from one edge and those from the other will be examined and the model modified, if necessary, to incorporate any changes of physical behavior detected.

## ACKNOWLEDGEMENT

We wish to thank Mr. W Sturrock of Defense Research Establishment Pacific for funding of this work.

## REFERENCES

- 1 Ying C.F. and Truell R., "Scattering of a Plane Longitudinal Wave by a Spherical Obstacle in an Isotropically Elastic Solid", *J. Appl. Phys.*, 27, 1956, pp 1086-1097.
- 2 Johnson G. and Truell R., "Numerical Computation of Elastic Scattering Cross Section", *J. Appl. Phys.*, 36, 1965, pp 3466-3475.
- 3 O'Neil H.T., "Theory of Focusing Radiators", *J. Acoust. Soc. Am.*, 21, 1949, pp 516-526.
- 4 Stockman A., Mathieu P., and Nicholson P.S., "Ultrasonic Characterization of Model Defects in Ceramics (Part 2): Spherical Oxide Inclusions in Glass - Theory and Practice", *Materials Evaluation*, 45, 1987, pp 736-742.  
Stockman A., Mathieu P., and Nicholson P.S., "Ultrasonic Characterization of Model Defects in Ceramics (Part 3): Spherical Inclusions in Opaque Crystallized Glass - Theory and Practice", *Materials Evaluation*, 47, 1989, pp 356-362.
- 5 Handbook of Chemistry and Physics, 59th edition, (Chemical Rubber Company Press, West Palm Beach Florida, 1978), p E-47.
- 6 Gaunard G.G., Tanglis E., Uberall H., Brill D., "Interior and Exterior Resonances in Acoustic Scattering I - Spherical Targets", *Il Nouvo Cimento*, 76B, 1983, pp 153-175.